

Syntheses of T_N building blocks *N*^α-(9-fluorenylmethoxycarbonyl)-*O*-(3,4,6-tri-*O*-acetyl-2-azido-2-deoxy-α-D-galactopyranosyl)-L-serine/L-threonine pentafluorophenyl esters: comparison of protocols and elucidation of side reactions[☆]

Mian Liu,^{a,b} Victor G. Young, Jr.,^{b,†} Sachin Lohani,^{c,†} David Live^{a,*} and George Barany^{b,*}

^aDepartment of Biochemistry, Molecular Biology and Biophysics, University of Minnesota, Minneapolis, MN 55455, USA

^bDepartment of Chemistry, University of Minnesota, Minneapolis, MN 55455, USA

^cDepartment of Pharmaceutics, University of Minnesota, Minneapolis, MN 55455, USA

Received 15 December 2004; accepted 22 February 2005

Available online 11 April 2005

Abstract—T_N antigen building blocks *N*^α-(9-fluorenylmethoxycarbonyl)-*O*-(3,4,6-tri-*O*-acetyl-2-azido-2-deoxy-α-D-galactopyranosyl)-L-serine/L-threonine pentafluorophenyl ester [Fmoc-L-Ser/L-Thr(Ac₃-α-D-GalN₃)-OPfp, **13/14**] have been synthesized by two different routes, which have been compared. Overall isolated yields [three or four chemical steps, and minimal intermediary purification steps] of enantiopure **13** and **14** were 5–18% and 6–10%, respectively, based on 3,4,6-tri-*O*-acetyl-*D*-galactal (**1**). A byproduct of the initial azidonitration reaction of the synthetic sequence, that is, *N*-acetyl-3,4,6-tri-*O*-acetyl-2-azido-2-deoxy-α-D-galactopyranosylamine (**5**), has been characterized by X-ray crystallography, and shown by ¹H NMR spectroscopy to form complexes with lithium bromide, lithium iodide, or sodium iodide in acetonitrile-*d*₃. Intermediates 3,4,6-tri-*O*-acetyl-2-azido-2-deoxy-α-D-galactopyranosyl bromide (**6**) and 3,4,6-tri-*O*-acetyl-2-azido-2-deoxy-β-D-galactopyranosyl chloride (**7**) were used to glycosylate *N*^α-(9-fluorenylmethoxycarbonyl)-L-serine/L-threonine pentafluorophenyl esters [Fmoc-L-Ser/L-Thr-OPfp, **11/12**]. Previously undescribed low-level dehydration side reactions were observed at this stage; the unwanted byproducts were easily removed by column chromatography.

© 2005 Elsevier Ltd. All rights reserved.

Keywords: Glycopeptide synthetic building blocks; Glycosylation; Side reactions; Metal ion–carbohydrate complexes; Dehydroalanine; Z-Dehydrothreonine

1. Introduction

In recent years, there has been an increased appreciation for the biological roles of mucin glycoproteins and glycoprotein domains. Quantitative studies of these glycoconjugates from natural sources have been challenging

for several reasons, including the microheterogeneity found naturally in their glycosylation.¹ Chemical synthesis has provided an alternative way to access well-defined glycopeptide structures that can be used to probe mucin glycoprotein properties.² This has been carried out either in solution,^{3,4} or (preferably for larger fragments) on solid supports.⁵ At present, the most efficient and versatile method for preparation of mucin-related *O*-linked glycopeptides, in particular those bearing the T_N antigens, uses protected glycosylated amino acids as building blocks in stepwise assembly.⁶ Facile and efficient procedures to prepare appropriately protected amino acid building blocks are therefore important to the practice of solid-phase glycopeptide synthesis. In

[☆] A preliminary report of portions of this work was presented at the 3rd International/28th European Peptide Symposium, Prague, Czech Republic, September 5–10, 2004.

* Corresponding authors. Tel.: +1 612 625 1028; fax: +1 612 626 7541 (G.B.); tel.: +1 612 626 3805; fax: +1 612 624 5121 (D.L.); e-mail addresses: david@nmrl.biochem.umn.edu; barany@umn.edu

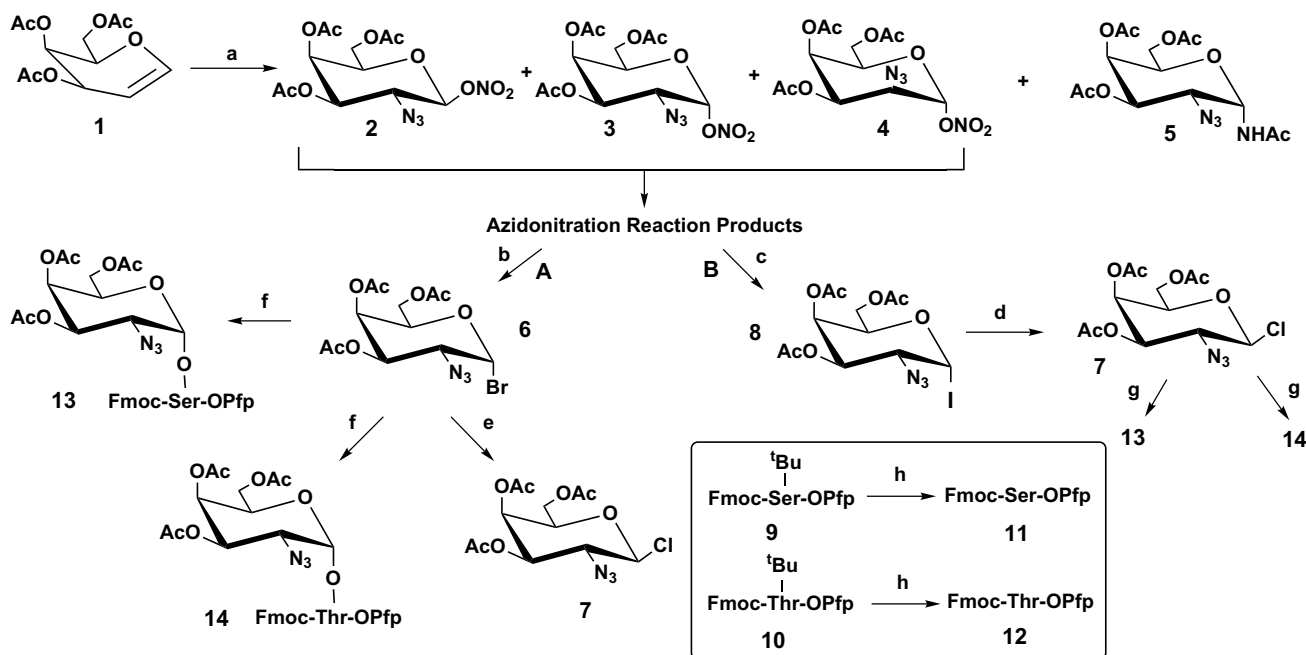
[†] These authors are responsible for the X-ray crystallographic analysis of compound **5**.

general, such building blocks are obtained by direct reaction of an *N*^α-9-fluorenylmethoxycarbonyl (Fmoc)-protected amino acid pentafluorophenyl (Pfp) ester with a glycosyl donor. Fmoc is preferred as an *N*^α-amino protecting group in peptide and glycopeptide synthesis since it is stable to glycosylation conditions. It can be removed during stepwise assembly under mild conditions with bases such as morpholine or piperidine, and it is stable to acidic conditions used in cleavage of glycopeptides from the support. Likewise, the Pfp ester serves a 'dual' function, insofar as it is stable and protects the C^α-carboxyl under conditions of glycosylation, while it provides activation of that same building block carboxyl group when needed for subsequent coupling. Prior syntheses of serine and threonine building blocks carrying galactosamine have been described and summarized.^{7–12} Here, we report some new findings on the syntheses of building blocks *N*^α-Fmoc-*O*-(3,4,6-tri-*O*-acetyl-2-azido-2-deoxy- α -D-galactopyranosyl)-L-serine/L-threonine pentafluorophenyl esters (**13/14**). By comparing protocols from the literature, those that are efficient and robust can be identified and recommended. The synthetic efforts reported here are part of a larger research program to probe by NMR spectroscopy the conformational properties of mucin glycopeptides, and are motivated in part by the need for optimal procedures that allow incorporation of isotopes as NMR probes.

2. Results and discussion

2.1. Syntheses of *N*^α-Fmoc-*O*-(3,4,6-tri-*O*-acetyl-2-azido-2-deoxy- α -D-galactopyranosyl)-L-serine/L-threonine pentafluorophenyl ester (**13/14**)

Two routes were used to synthesize the title building blocks (Scheme 1). Azidonitration of 3,4,6-tri-*O*-acetyl-D-galactal (**1**) under previously described conditions¹³ gave 3,4,6-tri-*O*-acetyl-2-azido-2-deoxy- β -D-galactopyranosyl nitrate (**2**), as well as the corresponding α -anomer **3** and the corresponding *tal*-isomer **4** [**2**:**3**:**4**, 1.0:1.25 (± 0.20):0.23 (± 0.03)]. The azidonitration reaction was monitored by reversed-phase high-performance liquid chromatography (RP-HPLC), and shown to be complete within 10 h at -20°C , as judged by disappearance of galactal **1**. Also produced under the conditions was *N*-acetyl-3,4,6-tri-*O*-acetyl-2-azido-2-deoxy- α -D-galactopyranosylamine (**5**) (similar level as **2**), as discussed in Section 2.2. The reaction mixture was transformed further, without purification of intermediates to 3,4,6-tri-*O*-acetyl-2-azido-2-deoxy- α -D-galactopyranosyl bromide (**6**) (Route A) or to 3,4,6-tri-*O*-acetyl-2-azido-2-deoxy- β -D-galactopyranosyl chloride (**7**) via α -iodide **8** (Route B). Either compound **6** or compound **7** was then coupled directly with *N*^α-(9-fluorenylmethoxycarbonyl)-L-serine/L-threonine pentafluorophenyl esters



Scheme 1. Synthetic routes to building blocks Fmoc-L-Ser/L-Thr(Ac₃- α -D-GalN₃)-OPfp (**13/14**). Reagents and conditions: (a) CAN, NaN₃, CH₃CN, -20°C , 10 h, 42% [following Ref. 13]; (b) LiBr, CH₃CN, 8 h, 82% [following Ref. 13]; (c) LiI, CH₃CN, 20 min, 48% [following Ref. 13]; (d) TEAC, CH₃CN, 25°C , 2.5 min, β : α = 5.5–6.8:1, 92% [following Ref. 13]; (e) TEAC, CH₃CN, 28°C for varying times, that is, β : α = 2.7:1 after 0.5 h and β : α = 1:2 after 1.5 h [following Ref. 17]; (f) Ag₂CO₃/AgClO₄, 1:1 toluene–CH₂Cl₂, molecular sieves (3 Å), N₂, in dark, reaction of **11** (48 h) gives **13** (50%) and reaction of **12** (24 h) gives **14** (28%) [following Ref. 11]; (g) Ag₂CO₃/AgClO₄, toluene–CH₂Cl₂ (1:1), molecular sieves (3 Å), N₂, in dark, reaction of **11** (4 days) gives **13** (23%) and reaction of **12** gives **14** (27%) [following Ref. 9]; (h) TFA, 92% for **11** (0.5 h reaction) and 95% for **12** (1 h reaction) [following Ref. 14].

(11/12)¹⁴ to give the corresponding α -glycosylated building blocks 13/14.^{9,11} According to the literature,¹⁵ the β -glycosyl chloride 7 was expected to induce higher α -stereoselectivity than the α -glycosyl bromide 6, a conclusion confirmed experimentally in the present study.

Route A (Scheme 1), involving three synthetic steps and two separations by silica gel chromatography, gave 13 and 14 in overall yields of 18% and 10%, respectively, based on 3,4,6-tri-*O*-acetyl-D-galactal (1). Route B (Scheme 1), involving four synthetic steps and two separations by silica gel chromatography, gave 13 and 14 in overall yields of 5% and 6%, respectively, also from 1. For the serine derivative 13, the α : β ratio—after glycosylation but before the final chromatography that removed residual β —was 6:1 and 4:1 by routes A and B, respectively. The poorer ratio in route B is attributable to the β : α ratio of 5.5:1 in 7, as discussed below; thus, route A is preferred. In either case, after regular silica gel chromatography, the pure building block 13 (>99% enantiopure) needed for glycopeptide synthesis was obtained. For the threonine derivative 14, route A via α -bromide 6 was preferred. About 10% of the β -anomer of 14 remained after standard silica gel chromatography, but further purification by normal-phase HPLC gave pure 14 (>99.9% enantiopure). In practice, 14 with \sim 10% of unwanted β was used for solid-phase glycopeptide synthesis. This did not create an insurmountable problem (Liu et al., submitted; see also Ref. 16), since the desired α -glycopeptides (even those containing three GalNAc-Thr units) were eventually readily separated, using RP-HPLC, from glycopeptides contaminated with one or more GalNAc-Thr β -anomers.

Note that there are two ways to access β -chloride 7. The method due to Lemieux and Ratcliffe¹³ (route B) uses α -iodide 8 as an intermediate and gave a ratio of β : α in the range of 5.5–6.8:1. Alternatively, compound 7 was obtained by treating pure 6 with tetraethylammonium chloride (TEAC) (route A). Under those reaction conditions, the α -stereoisomer was also generated. Ratios of β to α species were under kinetic control, that is, 2.7:1 after 0.5 h (the recommendation of Paulsen et al.¹⁷) 1:2 after 1.5 h, and 1:10 after 14 days at 25 °C. Thus, with time, the less stable β -chloride 7 isomerizes to its α -anomer; since the goal was to maximize formation of the β form, reactions were carried out as rapidly as possible, even without full conversion of 6.

2.2. X-ray crystallographic structure of *N*-acetyl-3,4,6-tri-*O*-acetyl-2-azido-2-deoxy- α -D-galactopyranosylamine (5)

Supporting what has been reported previously,^{13,18} we confirm that compound 5 is a byproduct formed, along with intended products 2, 3, and 4, during the azidonitration reaction (Scheme 1). Through use of ESIMS, we show here that compound 5 is *already* present in situ,

that is, prior to workup. Thus, while the pathway for generation of 5 must somehow involve water,¹³ this enters the nominally anhydrous reaction milieu at -20 °C. As a practical matter, even if compound 5 is formed—despite literature-described precautions to minimize its formation—it is readily separated by column chromatography. Indeed, we found that the fraction enriched in the mixture of 2, 3, and 4 [of which 2 and 3 are needed to continue on to the α -halo glycosylating agents 6 or 8] did not include any 5, as judged again by the ESIMS assay. That same chromatographic procedure did provide 5 in sufficient purity to allow its crystallization; such crystals were suitable for X-ray structural analysis (Figs. 1 and 2; Tables 1 and 2).

The molecules of 5 are found in the standard chair conformation in space group $P2_1$. The stereochemistry at C1 is clearly α . Bond lengths and angles are as expected (Table 2); in particular, the three nitrogens of the azide moiety are linear. After we solved the X-ray crystallographic structure of 5 in an anhydrous form at 173 K (spring 2004), another laboratory reported in this journal the structure of 5 in a monohydrate form, solved at 293 K.¹⁹ Both structures are monoclinic with the same space group, and have similar but not identical unit cell constants. Bond lengths and bond angles (Ref. 19 vs our Table 2) are the same, within experimental error. However, there are significant differences in the hydrogen-bonding pattern and in the packing, primarily due to inclusion of water. Indeed, the unit cell constants of the monohydrate form show an expansion parallel to the *a* axis. In our case, we find only one hydrogen bond: N1–H1B...O10 (Table 3), while in the monohydrate form, this hydrogen bond is broken with the concomitant insertion of water. The water oxygen in the literature structure accepts the acetylamide proton, while

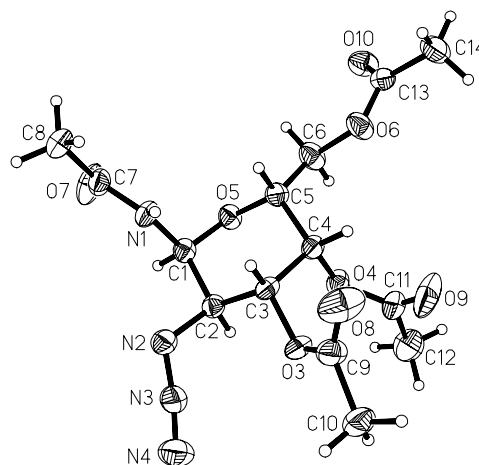


Figure 1. Thermal ellipsoid drawing, a numbering scheme for compound 5 as determined by X-ray crystallography. Both the azide (N2, N3, and N4) and one acetyl (O8, C9, C10) groups are disordered. The major occupancies of each were used in this drawing.

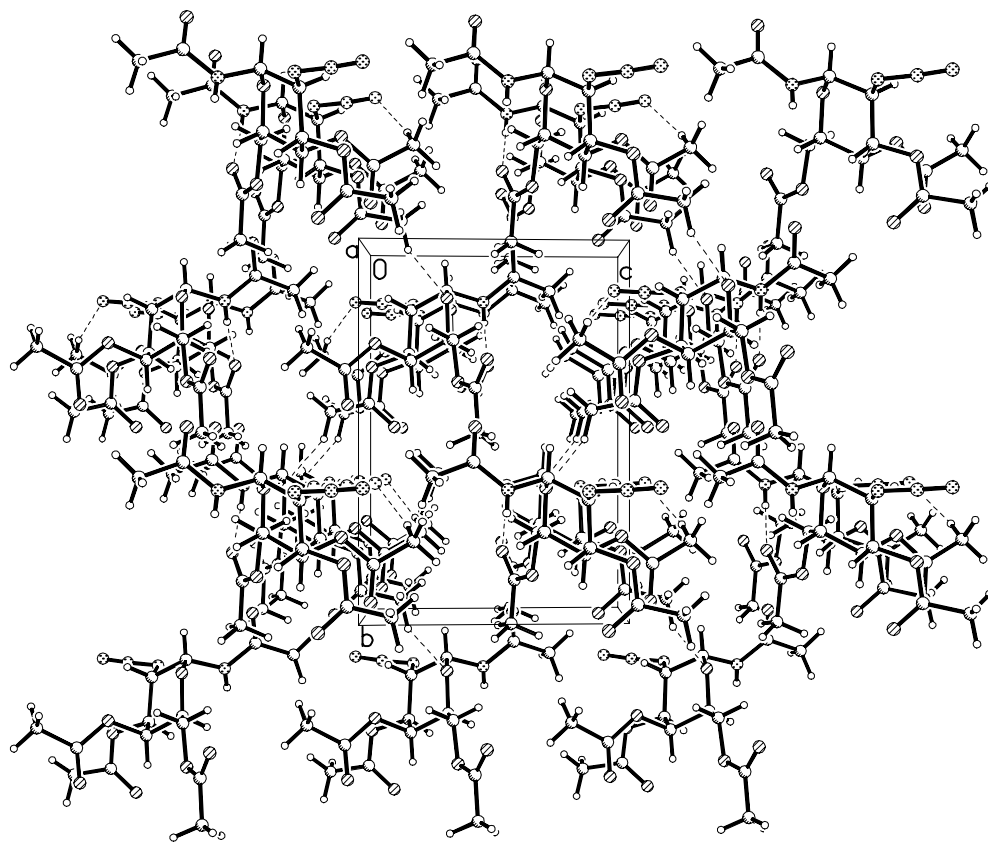


Figure 2. Molecular packing diagram of **5**, looking down the *b* axis.

Table 1. Selected X-ray crystallographic parameters for compound **5**

Empirical formula	C ₁₄ H ₂₀ N ₄ O ₈
Molecular weight	372.34
Space group	<i>P</i> 2 ₁
Unit cell dimensions	<i>a</i> = 8.2146(8) Å; <i>α</i> = 90° <i>b</i> = 12.5045(13) Å; <i>β</i> = 95.458(2)° <i>c</i> = 8.7710(9) Å; <i>γ</i> = 90°
<i>V</i> , Å ³	896.87(16)
<i>Z</i>	2
Density (calculated)	1.379 mg/mL
Absorption coefficient	0.114 mm ^{−1}
<i>F</i> (000)	392
Crystal color, morphology	Colorless, prisms
Crystal size	0.20 × 0.15 × 0.10 mm ³
<i>θ</i> Range for data collection	2.33–27.53°
Index ranges	−10 ≤ <i>h</i> ≤ 10, 0 ≤ <i>k</i> ≤ 16, 0 ≤ <i>l</i> ≤ 11
Reflections collected	9120
Independent reflections	2146 [<i>R</i> (int) = 0.0282]
Observed reflections [<i>I</i> ≥ 2σ(<i>I</i>)]	2007
Completeness to <i>θ</i> = 27.53°	99.3%
Data/restraints/parameters	2146/7/257
Goodness-of-fit on <i>F</i> ^{2,a}	1.061
Final <i>R</i> indices [<i>I</i> > 2σ(<i>I</i>)]	^b <i>R</i> ₁ = 0.0396, ^b <i>wR</i> ₂ = 0.0977
<i>R</i> Indices (all data)	^c <i>R</i> ₁ = 0.0428, ^b <i>wR</i> ₂ = 0.1001
Largest diff. peak and hole	0.340 and −0.278 e Å ^{−3}

$$^a \text{GooF} = S = \left[\frac{\sum [w(F_o^2 - F_c^2)^2]}{(n - p)} \right]^{1/2}.$$

$$^b R_1 = \frac{\sum ||F_o| - |F_c||}{\sum |F_o|}.$$

$$^c wR_2 = \left[\frac{\sum [w(F_o^2 - F_c^2)^2]}{\sum [w(F_o^2)^2]} \right]^{1/2}.$$

$$w = q / [\sigma^2(F_o^2) + (a^*P)^2 + b^*P + d + e^* \sin(\theta)].$$

making two additional hydrogen bonds with acetyl oxygens on neighboring molecules [the authors did not explicitly locate the water protons, but the reported O···O contacts of 2.500(6) and 2.608(8) Å are strongly consistent with such an interpretation].¹⁹ In comparing the two structures, it might appear that the monohydrate form should be more stable, since no disorder was found, while the anhydrous form exhibited disorder in one of the acetyl groups and in the azide.

As indicated in Section 2.3, knowledge of the structure of **5** helps to provide a basis for why the next step in the overall preparative process (Scheme 1) may be simplified by eliminating separation of **5** from the mixture before proceeding with further synthetic steps.

2.3. Discovery of lithium and sodium ion binding properties of *N*-acetyl-3,4,6-tri-*O*-acetyl-2-azido-2-deoxy-α-D-galactopyranosylamine (**5**)

To determine if the presence of byproduct **5** would have an adverse effect on conversion of the azidonitration product mixture to α-halo glycosylating agents, we decided, with pure **5** in hand, to investigate particularly its interaction with the salts, that is, lithium bromide and lithium iodide, used in this conversion (Scheme 1), as well as with sodium iodide as a control. These investigations used ¹H NMR spectroscopy (Fig. 3; Table 4).

Table 2. Selected bond lengths (Å) and bond angles (°) for compound **5**

C1–C2	1.528(3)	O5–C1–C2	108.95(18)
O5–C1	1.427(3)	C3–C2–C1	111.60(18)
C3–C2	1.528(3)	C3–C2–N2	110.7(2)
C2–N2	1.479(3)	C1–C2–N2	108.55(18)
N2–N3	1.228(3)	N2–N3–N4	172.7(5)
N3–N4	1.122(4)	C4–C3–C2	110.68(19)
N3'–N4'	1.121(5)	O3–C3–C2	106.01(18)
C3–C4	1.526(3)	C3–C4–C5	108.21(18)
O3–C3	1.444(3)	O4–C4–C3	108.69(18)
C4–C5	1.528(3)	O5–C5–C4	110.74(19)
O4–C4	1.446(3)	O5–C5–C6	103.60(19)
C5–C6	1.514(3)	C5–C6–O6	108.0(2)
O5–C5	1.432(3)	N1–C1–C2	112.75(19)
C6–O6	1.440(3)	N1–C7–O7	122.0(2)
O3–C9	1.313(5)	N1–C7–C8	115.4(2)
O3–C9'	1.382(9)	C9–O3–C9'	35.3(4)
O8–C9	1.195(5)	C9'–O3–C3	121.1 (4)
O8'–C9'	1.206(10)	C9–O3–C3	118.4(2)
C9–C10	1.493(7)	O8–C9–O3	122.7(4)
C9'–C10'	1.491(14)	O8'–C9'–O3	121.5(7)
N1–C1	1.440(3)	O8–C9–C10	125.3(7)
N1–C7	1.359(3)	O8'–C9'–C10'	125.8(14)

Table 3. Hydrogen bonding in compound **5**

D–H···A	<i>d</i> (D–H) (Å)	<i>d</i> (H···A) (Å)	<i>d</i> (D···A) (Å)	<(DHA) (°)
N1–H1B···O10 ^a	0.88	2.18	3.009(3)	157.5

^a Symmetry transformations used to generate equivalent atoms: $x - 1, y, z$. D is donor, A is acceptor.

Compound **5** was subjected to the conditions used in the preparation of α -bromide **6** or α -iodide **8** (Scheme 1), and then reisolated by an extractive workup. From the superimposability of spectra (Fig. 3), recorded in acetonitrile- d_3 before or after exposure to lithium bromide, lithium iodide, or sodium iodide, it was concluded that no significant reactions occur between ions and sugar **5**. The α configuration of the sugar is retained upon interactions with metal ions. As a practical point, then, it was possible to take the *entire* azidonitration product mixture, which includes about 30 mol % of **5**, and carry out the subsequent reaction. Nevertheless, the amount of salts needed for full conversion of **2** and **3** had to

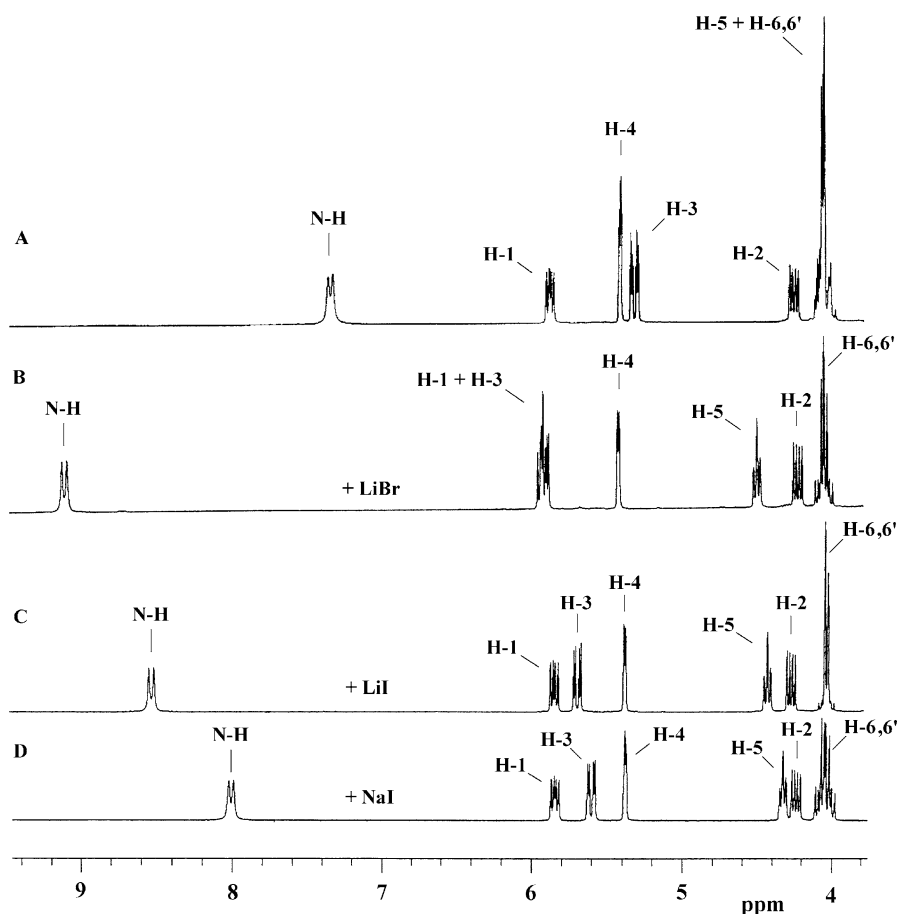


Figure 3. ^1H NMR spectra of compound **5** in acetonitrile- d_3 . Chemical shift assignments were determined based on 2D COSY spectra. Panel A: Compound **5**, after purification from among the products of the azidonitration reaction. Note that when pure **5** was subjected to reaction conditions involving LiBr, LiI, or NaI (details in text), following which, the reaction was quenched, organic product was extracted into CH_2Cl_2 , while aqueous washes removed the salts, and the organic phase was concentrated, and the residue was dissolved in acetonitrile- d_3 , the NMR spectrum was superimposable on the one now shown in Panel A; Panel B: Compound **5** (40 mM) and LiBr (5 equiv) were mixed; Panel C: the same, but with 7 equiv of LiI; Panel D: the same, but with 5 equiv of NaI.

Table 4. Chemical shift increments (δ : ppm) of compound **5** in the presence of lithium bromide, lithium iodide, or sodium iodide in acetonitrile- d_3 ^{a,b}

Compound 5	N–H	H-3	H-5	H-1	H-2	H-4	H-6
In CD ₃ CN	7.30	5.30	4.06	5.85	4.25	5.39	4.06
Increment (+ LiBr)	1.75	0.59	0.43	0.04	–0.03	0.01	–0.01
Increment (+ LiI)	1.22	0.38	0.36	–0.02	0.01	–0.03	–0.03
Increment (+ NaI)	0.71	0.30	0.26	–0.01	–0.02	–0.01	0

^a Significant increments are shown in boldface for emphasis.

^b The effects of sodium bromide, potassium bromide, and potassium iodide could not be evaluated, because of the limited solubility of these salts in acetonitrile- d_3 .

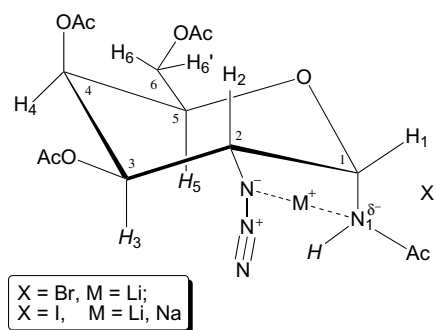
be increased [e.g., in the case of LiBr, from 1.2 to 1.8 mass equiv] when **5** was also present. After the reaction was complete, superfluous **5** was readily removed by column chromatography.

NMR spectra of **5** in acetonitrile- d_3 were then recorded in situ, in the presence of salts [LiBr, LiI, or NaI; Fig. 3, Table 4]. In all cases, significant changes in chemical shifts of **5** were induced at the N–H, H-3, and H-5 sites, while the shift effects on H-1, H-2, H-4, and H-6, among others, were negligible. These NMR data are consistent with binding of the alkali ion by sugar **5**, and make it possible to pinpoint the molecular contacts.

The NMR-suggested formation of complexes of lithium or sodium ions with **5** was supported further by ESIMS data (Table 5). When **5** was mixed with lithium or sodium salts, mass spectra show as the base peaks the expected 1:1 adducts. Interpretation of the results are complicated somewhat by the control spectra of **5** alone, which showed significant levels of metal:cation adducts, for cation plus sodium or potassium adsorbed from the external medium; even ions consisting of **5** plus cation in a 2:1 ratio were observed. Nevertheless, the data are clearly consistent with a strong affinity of sugar **5** to alkali cations.

With the X-ray structure (Figs. 1 and 2) and NMR results (Table 4) of **5** in hand, we were in a position to develop a more specific understanding of how the alkali metal ions interact with the protected carbohydrate. While other examples of metal–carbohydrate complexes have been reviewed,^{20–24} these all differ from **5** insofar as free hydroxyl groups are available for coordination with metal ions.

The X-ray structural data on the disposition of functional groups was taken into account to develop a model (Fig. 4) for the likely contact points of alkali cation

**Figure 4.** Proposed model for complex of compound **5** with LiBr, LiI, or NaI. Significant chemical shifts changes observed for N–H, H-3, and H-5 are consistent with their proximity to the metal cation. The resonance structure of the azide group shown in the above is arbitrary.

binding by azide-containing sugar **5** in a polar aprotic organic solvent. Both the lone pair of nitrogen N1 and the azide group are involved, but none of the oxygens of the *O*-acetyl protected hydroxyl groups participate in metal binding. Also, H-3 and H-5 are in close proximity to the cation, consistent with the experimentally observed downfield chemical shifts diagnostic of significant deshielding. H-5 is not as close to the cation as H-3, so the deshielding of the former is less than that of the latter. It was also determined, from NMR data, that the maximal cation interaction was with lithium, and the maximal anion interaction was with bromide. Thus, the chemical shift changes of N–H (1.22 vs 0.71), H-3 (0.38 vs 0.30), and H-5 (0.36 vs 0.26) are greater with lithium (iodide) than with sodium (iodide); and comparing N–H (1.75 vs 1.22), H-3 (0.59 vs 0.38), and H-5 (0.43 vs 0.36) shows how the effects of (lithium) bromide are greater than those of (lithium) iodide (Table 4). While alkali metals and **5** do not undergo chemical reactions, the fact that they are coordinated explains why

Table 5. Mass spectrometric characterization of complexes of **5** with lithium bromide, lithium iodide, and sodium iodide^a

Compound 5	Compound 5 + LiBr	Compound 5 + LiI	Compound 5 + NaI
373.1 (6) [M+H] ⁺	379.1 (100) [M+Li] ⁺	379.1 (100) [M+Li] ⁺	395.1 (100) [M+Na] ⁺
395.1 (100) [M+Na] ⁺	751.3 (8) [2M+Li] ⁺		
411.1 (51) [M+K] ⁺			
767.2 (20) [2M+Na] ⁺			
783.2 (6) [2M+K] ⁺			

^a Compound **5** plus salt were dissolved in methanol and subjected to ESIMS. The Table reports *m/z* in the positive mode of the major monoisotopic peaks in each spectrum, followed by relative intensity (within parentheses) and assignment [within brackets].

additional salt must be present when **5** is carried through to the next step.

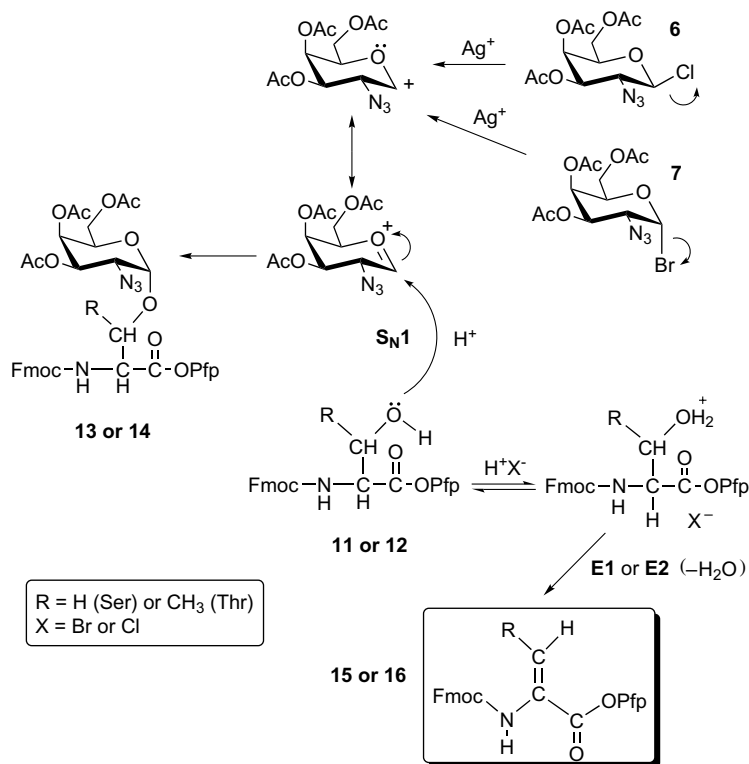
2.4. Dehydration reaction during glycosylation of *N*^α-(9-fluorenylmethoxycarbonyl)-L-serine/L-threonine pentafluorophenyl esters (**11/12**)

During the reactions of *N*^α-(9-fluorenylmethoxycarbonyl)-L-serine/L-threonine pentafluorophenyl esters (**11/12**) with 3,4,6-tri-*O*-acetyl-2-azido-2-deoxy- α -D-galactopyranosyl bromide (**6**) or 3,4,6-tri-*O*-acetyl-2-azido-2-deoxy- β -D-galactopyranosyl chloride (**7**), dehydration products *N*^α-(9-fluorenylmethoxycarbonyl)-dehydroalanine/dehydrothreonine pentafluorophenyl esters (**15/16**) formed at low yields [Scheme 2: 2% and 5% of **15** in Ser family; 3% and 4% of **16** in Thr family with glycosylated donors **6** and **7**, respectively]. Mechanistically, we hypothesize that the dehydration reactions are catalyzed by the acids, hydrogen bromide, and hydrogen chloride, which are generated during glycosylation. Thus, bromide and chloride ions are leaving groups from **6** and **7**, with assistance of Ag⁺ ions. After combining with protons released from **11** and **12**, the haloacids could recombine with hydroxyl groups on **11** and **12**, and then form dehydrated byproducts **15** and **16** by E1 or E2 procedures. This competes with formation of building blocks **13** and **14**, which are products of Königs–Knorr α -glycosylation reactions that follow an S_N1

mechanism. Note that hydrogen chloride catalyzes the dehydration reaction more efficiently than hydrogen bromide.

As a control, compounds **9** and **10** were exposed to trifluoroacetic acid (TFA), which resulted in effective removal of *tert*-butyl ether side-chain protection without any kind of dehydration reaction, as evidenced by ESIMS (spectra not shown) and RP-HPLC (Fig. 5).

The geometry of the double bond of Thr-derived dehydration product **16** was investigated by a 1D nuclear Overhauser enhancement (1D NOE) experiment (Fig. 6). Selective excitation of the methyl group at 1.91 ppm provided enhanced signals on the NH proton at 6.16 ppm, Fmoc-CH₂ protons at 4.51 ppm, Fmoc-CH proton at 4.27 ppm, and Ar-H proton at 7.60 ppm (Panel B). However, saturation of the NH proton at 6.16 ppm did not yield observable NOE enhancement, perhaps due to difficulty in saturating the broad peak. These data revealed that a single stereoisomer of dehydrothreonine ester was formed, that is, compound **16**, which has a *Z* geometry. The existence of the *Z* isomer was further demonstrated when saturation of the olefinic quartet at 7.22 ppm in the NOE experiment did not yield any enhancement except for the methyl group at 1.91 ppm (Panel C). The exquisite stereospecificity of the Thr dehydration was observed previously in another context, and established by similar 1D NOE experimental analysis.²⁵



Scheme 2. Proposed mechanism for the dehydration of Fmoc-L-Ser/L-Thr-OPfp (**11/12**) as a side reaction during the intended reaction of **6** or **7** with **11/12** to provide **13/14**.

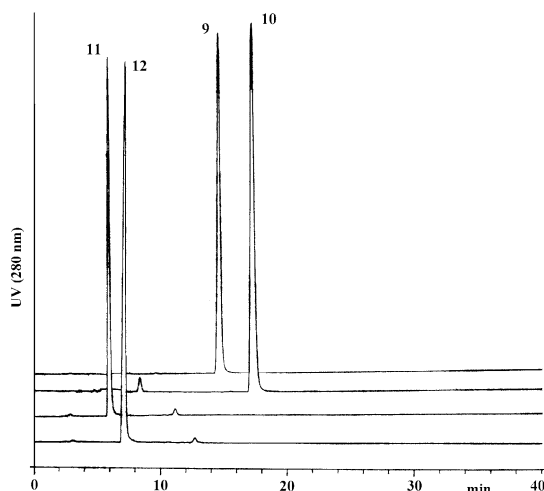


Figure 5. RP-HPLC profiles of **9**, **10**, **11**, and **12**. The four panels show, respectively (top to bottom): Fmoc-Ser(^tBu)-OPfp (**9**) (t_R 14.6 min); Fmoc-Thr(^tBu)-OPfp (**10**) (t_R 17.2 min); Fmoc-Ser-OPfp (**11**) (t_R 6.1 min); and Fmoc-Thr-OPfp (**12**) (t_R 7.0 min). Compounds **11** and **12** are the products from TFA-mediated deprotections of **9** and **10**, and were detected directly by RP-HPLC analysis. Retention times of dehydration products **15** and **16** are 14.6 and 11.7 min, respectively (RP-HPLC profiles not shown). Analytical RP-HPLC column (C_{18} : 4.6×250 mm) with detection at 280 nm, linear gradients of 0.1% aqueous TFA (Buffer A) and 0.1% TFA in CH_3CN (Buffer B) were run at a 1.0 mL/min flow rate from 60% to 100% B over 40 min.

3. Conclusions

This paper compares several approaches to the preparation of Fmoc-L-Ser/L-Thr(Ac_3 - α -D-GalN₃)-OPfp (**13**/**14**), building blocks for glycopeptides synthesis. The desired pure α -anomer of serine is obtained readily, with the final stage being regular silica gel chromatography. However, in the threonine family, isolation of enantiopure α -anomer **14** requires normal-phase HPLC. The initial azidonitration reaction gives a mixture of products, including the byproduct, *N*-acetyl-3,4,6-tri-*O*-acetyl-2-azido-2-deoxy- α -D-galactopyranosylamine (**5**), the structure of which has been confirmed by X-ray crystallography. 1H NMR studies reveal that **5** can bind to lithium or sodium cations, and a model to explain these results has been proposed. Structural and mechanistic insights garnered throughout this work have led to streamlined, practical syntheses of intermediates, and final building blocks.

4. Experimental

4.1. General methods

Solvents and reagents were of the highest commercially available grade, and generally used directly as obtained from Aldrich Chemical Co. (Milwaukee, WI), ICN Bio-medicals (Aurora, OH), or Alfa Aesar (Wardhill, MA). However, CH_2Cl_2 and toluene were freshly distilled

from anhyd CaH_2 before use, and MeOH was maintained over 3 Å molecular sieves. *N*^z-Fmoc-L-Ser(^tBu)-OPfp (**9**) and *N*^z-Fmoc-L-Thr(^tBu)-OPfp (**10**) were obtained from BACHEM (San Carlos, CA), and 3,4,6-tri-*O*-acetyl-D-galactal was obtained from Aldrich. TLC was carried out on E. Merck Silica Gel 60 F₂₅₄ on aluminum sheets, and visualized by charring with 10% sulfuric acid in ethanol and/or by UV light (254 nm), as appropriate. Regular silica gel chromatography was performed on silica gel (70–230 mesh) using hexanes (92% *n*-hexane, obtained from Mallinckrodt Laboratory Chemicals, Phillipsburg, NJ) and EtOAc for elution. Analytical RP-HPLC was performed using a Vydac C_{18} reversed-phase column (4.6×250 mm) on a Beckman instrument configured with two model 112 pumps and a model 165 variable wavelength detector, eluted at a 1.0 mL/min flow rate by linear gradients of 0.1% aqueous TFA (Buffer A) and 0.1% TFA in CH_3CN (Buffer B) over 40 min. Preparative normal-phase HPLC was performed using a silica gel column (21.4×250 mm) with an integrated guard module on a Beckman instrument configured with a model 125P solvent module and a model 166P detector (set at 280 nm), eluted at a 15 mL/min flow rate by an isocratic mixture of 4:1 hexanes–EtOAc. NMR spectra were recorded, with $CDCl_3$ as solvent, on Varian Inova instruments operating for 1H at 300, 500, or 600 MHz and for ^{13}C at 125 MHz. The reported chemical shifts were referenced to Me_4Si and are considered accurate to ± 0.02 (1H) and ± 0.5 (^{13}C). Electrospray ionization-mass spectrometry (ESIMS) was performed on a Bruker BioTOF II instrument in the University of Minnesota Department of Chemistry, with samples being introduced via direct infusion with a syringe pump.

4.2. Azidonitration of 3,4,6-tri-*O*-acetyl-D-galactal

Following Lemieux and Ratcliffe¹³ a solution of 3,4,6-tri-*O*-acetyl-D-galactal (**1**) (2.11 g, 7.7 mmol) in CH_3CN (42 mL) was added dropwise over 5 min to a vigorously stirred mixture of solid sodium azide (0.75 g, 11.5 mmol) and solid ceric ammonium nitrate (CAN, 12.65 g, 28.1 mmol) at $-20^\circ C$. To achieve and maintain this temperature, the reaction vessel was immersed in a brine solution that was in turn surrounded by powdered dry ice. Starting material **1** (t_R = 26.7 min) disappeared within 10 h, as monitored by RP-HPLC (0–40% Buffer B over 40 min, detection at 225 nm). Aliquots were also taken for ESIMS evaluation. The reaction was quenched by adding cold Et_2O (50 mL) and water (50 mL). The organic layer was separated and washed with ice-cold water (3×50 mL), and dried ($MgSO_4$). Evaporation of the solvent left a yellow syrup (2.0 g), which will be referred to as ‘crude azidonitration reaction product mixture’. For some of the goals of this research, the ‘crude mixture’ could be used successfully as a starting point for further

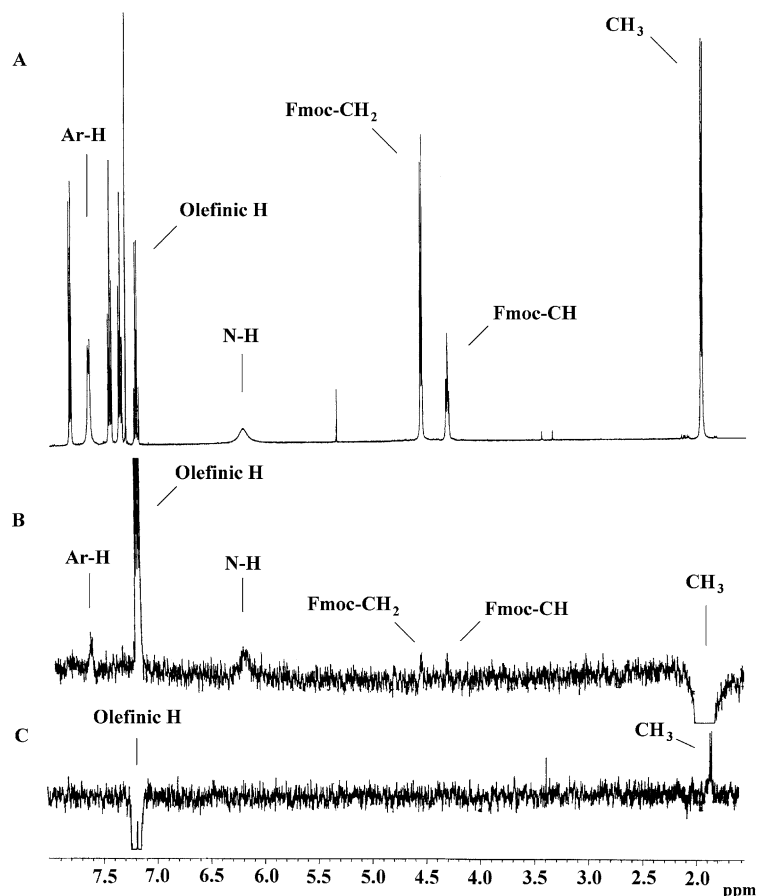


Figure 6. NMR experiments to establish the stereochemistry of compound **16**. Panel A, ^1H NMR spectrum of **16**. Panel B, after the methyl group has been selectively excited. Panel C, after the olefinic proton has been selectively excited.

transformations. In other cases, the ‘crude mixture’ (2.0 g) was dissolved in 3:2 hexanes–EtOAc (10 mL) and applied to a silica gel column (16 \times 3 cm) that had been pre-equilibrated with hexanes. The chromatogram was eluted with 3:2 hexanes–EtOAc to provide two fractions. The first fraction (1.2 g, 42%) proved to be a mixture of azidonitration products: 3,4,6-tri-*O*-acetyl-2-azido-2-deoxy- β -D-galactopyranosyl nitrate (**2**), α -anomer **3**, and *talo*-isomer **4**; ratios of compounds **2**, **3**, and **4** were typically 1:1.25(\pm 0.20):0.23(\pm 0.03), as determined by the relative intensities of the diagnostic ^1H NMR shifts assigned to anomeric protons. R_f 0.48 (3:2 hexanes–EtOAc). ESIMS: m/z 415.1 $[\text{M}+\text{K}]^+$, 399.1 $[\text{M}+\text{Na}]^+$. This first chromatography fraction will be referred to as ‘chromatographed azidonitration reaction product **2/3/4** mixture’.

The second chromatographic fraction (0.5 g, 17%) was determined to be *N*-acetyl-3,4,6-tri-*O*-acetyl-2-azido-2-deoxy- α -D-galactopyranosylamine (**5**). R_f 0.21 (2:1 hexanes–EtOAc). Compound **5** was precipitated from anhyd Et_2O , and then redissolved in hot Et_2O . After filtration, the filtrate was brought to a brief boil, and then allowed to cool slowly to 25 $^\circ\text{C}$. Crystals ap-

peared within a few hours, and further crystal growth was allowed to proceed for 2 days. ESIMS: m/z 783.2 $[\text{2M}+\text{K}]^+$, 767.2 $[\text{2M}+\text{Na}]^+$, 411.1 $[\text{M}+\text{K}]^+$, 395.1 $[\text{M}+\text{Na}]^+$, 373.1 $[\text{M}+\text{H}]^+$. ^1H NMR data of **2–5** were in agreement with those previously reported.^{13,19}

4.3. 3,4,6-Tri-*O*-acetyl-2-azido-2-deoxy- α -D-galactopyranosyl bromide (**6**)

4.3.1. Initial method. Again following Lemieux and Ratcliffe¹³ ‘chromatographed azidonitration reaction product **2/3/4** mixture’ (1.2 g, 3 mmol) was treated with a suspension of LiBr (1.3 g, 15 mmol) in CH_3CN (11 mL) at 25 $^\circ\text{C}$ for 8 h, with reaction progress being monitored by ESIMS. The reaction mixture was diluted with CH_2Cl_2 (100 mL) and water (2 \times 50 mL), and the organic phase was concentrated and applied to a regular silica gel column (12 \times 4 cm). Elution with 1:0 \rightarrow 1:1 hexanes–EtOAc provided the title product as a syrup (0.96 g, 2.42 mmol, 82%). R_f 0.66 (1:1 hexanes–EtOAc). The ^1H NMR data of this syrup agreed with earlier reports¹³ and did not change for over a month of storage at 4 $^\circ\text{C}$. ^{13}C NMR (125 MHz, CDCl_3): 170.4

(C6–O–C=O), 169.8 (C4–O–C=O), 169.6 (C3–O–C=O), 89.0 (C1), 71.5 (C5), 69.9 (C3), 66.6 (C4), 60.8 (C6), 58.7 (C2), 20.6–20.7 (3CH₃). ESIMS: m/z 432.0 [M+K]⁺, 416.0 [M+Na]⁺, 394.1 [M+H]⁺.

4.3.2. Preferred method. The ‘crude azidonitration reaction product mixture’ (0.51 g, 1.35 mmol), together with LiBr (0.6 g, 7.0 mmol), was suspended in CH₃CN (5 mL). The mixture was stirred at 25 °C for 8 h, following which the product was isolated by techniques already described in the immediately preceding section. A syrup (125 mg) was obtained, which comprised product **6**, together with unreacted starting materials **2**, **3**, and **4** (1:0.42:0.78:0.20), as detected and quantified by NMR [note that **5**, though present, was not detected by NMR in CDCl₃, as first remarked on in Ref. 13]. The syrup was dissolved again in CH₃CN (5 mL), LiBr (0.6 g) was added, and stirring proceeded for 4 h. The reaction mixture was diluted with CH₂Cl₂ (10 mL), washed with water (2 × 5 mL), and then the organic phase was dried (NaSO₄), filtered, and concentrated to provide the title compound (124 mg, ~60%). Alternatively, a solution of the ‘crude azidonitration reaction product mixture’ (1.0 g, ~2.7 mmol) in CH₃CN (10 mL) with LiBr (1.8 g, 21 mmol) was stirred at 25 °C for 8 h. The product was isolated as described in Section 4.3.1 to provide the title compound (354 mg, 80%).

4.4. 3,4,6-Tri-*O*-acetyl-2-azido-2-deoxy-β-D-galactopyranosyl chloride (**7**)

4.4.1. Initial method. Following Paulsen et al.,¹⁷ a solution of compound **6** (20 mg, 50 μmol) in CH₃CN (1.5 mL) was added to a 0.12 M solution of TEAC in CH₃CN (1.5 mL) at 28 °C. After 1.5 h, the reaction mixture was diluted with toluene (14.5 mL), washed with water (2 × 5 mL), and dried (Na₂SO₄). ¹H NMR (300 MHz, CDCl₃) revealed that β:α = 1:2. For β-anomer **7**: δ 5.11 (d, 1H, $J_{1,2}$ 9.0 Hz, H-1), 4.84 (q, 1H, $J_{2,3}$ 10.5 Hz, $J_{3,4}$ 3.3 Hz, H-3), 3.87 (q, 1H, H-2), 2.20, 2.08, 2.06 (3s, 9H, 3CH₃). For α-anomer: δ 6.19 (d, 1H, $J_{1,2}$ 3.6 Hz, H-1), 5.52 (q, 1H, $J_{4,5}$ 1.2 Hz, $J_{3,4}$ 3.3 Hz, H-4), 5.39 (q, 1H, $J_{2,3}$ 10.8 Hz, H-3), 2.18, 2.08, 2.07 (3s, 9H, 3CH₃). ESIMS: m/z 372.1 [M+Na]⁺, 350.1 [M+H]⁺, 314.1 [M–Cl]⁺. When the same material (already worked up) was rechecked after 14 days at 25 °C, the β:α ratio was 1:10. When the same reaction was carried out for 0.5 h at 28 °C, the β:α ratio after workup was 2.7:1.

4.4.2. Preferred method. Again following Lemieux and Ratcliffe¹³ 3,4,6-tri-*O*-acetyl-2-azido-2-deoxy-α-D-galactopyranosyl iodide (**8**) (1.13 g, 48%) in the form of a yellow foam was obtained from the ‘chromatographed azidonitration reaction product **2/3/4** mixture’ and evaluated by ¹H NMR spectroscopy (300 MHz, CDCl₃): δ

6.82 (d, 1H, $J_{1,2}$ 4.2 Hz, H-1), 5.46 (d, 1H, $J_{3,4}$ 3.2 Hz, H-4), 5.18 (q, 1H, $J_{2,3}$ 10.7 Hz, H-3), 3.40 (q, 1H, H-2), 2.15, 2.05, 2.00 (3s, 9H, 3CH₃). ESIMS: m/z 479.9 [M+K]⁺, 464.0 [M+Na]⁺. Treatment of this yellow foam with TEAC by the procedure just alluded to provided a mixture of both chloride anomers (0.82 g, 92%, β:α = 5.5–6.8:1).

4.5. *N*-(9-Fluorenylmethoxycarbonyl)-L-serine pentafluorophenyl ester (**11**)

Following Bock and co-workers¹⁴ compound **9** (4.54 g, 8.26 mmol) was treated with TFA (80 mL) for 30 min at 25 °C. The reaction solution was concentrated to dryness in vacuo and coevaporated with toluene (2 × 30 mL) to provide the title compound **11** (3.75 g, 7.6 mmol, 92%). t_R 6.1 min (60–100% Buffer B over 40 min, detection at 280 nm). ¹H NMR (300 MHz, CDCl₃):²⁶ δ 7.74, 7.57, 7.38, 7.28 (8H, Ar–H), 5.93 (d, 1H, J_{NH-CH^a} 7.2 Hz, NH), 4.39–4.51 (m, 2H, CH^B), 4.18–4.22 (m, 3H, CH^a, Fmoc–CH₂), 4.00 (q, 1H, J_1 11.3 Hz, J_2 2.7 Hz, Fmoc–CH). The proton signal due to N–H was suppressed by addition of a drop of D₂O. ESIMS: m/z 532.1 [M+K]⁺, 516.1 [M+Na]⁺, 494.1 [M+H]⁺.

4.6. *N*-(9-Fluorenylmethoxycarbonyl)-L-threonine pentafluorophenyl ester (**12**)

Following Bock and co-workers¹⁴ compound **10** (4.0 g, 6.96 mmol) was treated with TFA (35 mL) for 1 h at 25 °C. The reaction solution was concentrated to dryness in vacuo and coevaporated with toluene (2 × 30 mL) to provide the title compound **12** (3.34 g, 6.59 mmol, 95%). t_R = 7.0 min (60–100% Buffer B over 40 min at 280 nm). ¹H NMR (300 MHz, CDCl₃):²⁶ δ 7.79, 7.63, 7.42, 7.33 (8H, Ar–H), 5.71 (d, 1H, J_{NH-CH^a} 9.6 Hz, NH), 4.73 (q, 1H, $J_{CH^a-CH^B}$ 1.8 Hz, CH^a), 4.59–4.61 (m, 1H, CH^B), 4.50 (q, 2H, $J_{FmocCH_2-FmocCH_2}$ 2.4 Hz, Fmoc–CH₂), 4.27 (t, 1H, $J_{FmocCH-FmocCH_2}$ 6.9 Hz, Fmoc–CH), 2.04 (br, 1H, OH), 1.36 (d, 3H, $J_{CH_3-CH^B}$ 6.3 Hz, CH₃). Proton signals of N–H and O–H were suppressed by addition of a drop of D₂O. ESIMS: m/z 546.1 [M+K]⁺, 530.1 [M+Na]⁺, 508.1 [M+H]⁺.

4.7. *N*-(9-Fluorenylmethoxycarbonyl)-*O*-(3,4,6-tri-*O*-acetyl-2-azido-2-deoxy-α-D-galactopyranosyl)-L-serine pentafluorophenyl ester (**13**)

4.7.1. Method A. Following Levine and co-workers¹¹ a solution of **11** (80 mg, 0.16 mmol) in dry 1:1 toluene–CH₂Cl₂ (10 mL) was stirred with Ag₂CO₃ (100 mg, 0.36 mmol), AgClO₄ (15 mg, 0.066 mmol), and molecular sieves (215 mg, 3 Å, powdered), in the dark and under N₂, at 20 °C for 12 h. Next, a solution of compound **6** (96 mg, 0.25 mmol) in dry 1:1 toluene–CH₂Cl₂ (2 mL) was added dropwise over 1 h, and the stirring was

continued for 48 h. Then, the mixture was diluted with CH_2Cl_2 (40 mL) and filtered through dry Celite (~2 g) and concentrated, and the filtrate was washed with 5% aq NaHCO_3 (3×10 mL) followed by water (2×10 mL). The organic layer was dried over anhyd Na_2SO_4 and concentrated in vacuo to dryness and subjected to standard silica gel chromatography with 4:1 hexanes–EtOAc for elution, whereupon three fractions were collected. Fraction A (1.6 mg, 2%) was Fmoc–dehydroalanine pentafluorophenyl ester (**15**). R_f 0.83 (1:1 hexanes–EtOAc). ^1H NMR (500 MHz, CDCl_3): δ 7.78 (d, 2H, J 7.5 Hz, Ar–H), 7.63 (d, 2H, J 7.5 Hz, Ar–H), 7.45 (m, 2H, Ar–H), 7.36 (m, 2H, Ar–H), 7.09 (s, 1H, CH_a), 6.57 (br, 1H, NH), 6.17 (s, 1H, CH_b), 4.52 (d, 2H, J 6.9 Hz, Fmoc– CH_2), 4.27 (t, 1H, Fmoc–CH). ESIMS: m/z 514.1 $[\text{M}+\text{K}]^+$, 498.1 $[\text{M}+\text{Na}]^+$. Fraction B was title compound **13** (65 mg, 50%). R_f 0.51 (1:1 hexanes–EtOAc). ^1H NMR data were in agreement with those previously reported.⁹ ESIMS: m/z 845.2 $[\text{M}+\text{K}]^+$, 829.2 $[\text{M}+\text{Na}]^+$, 807.2 (MH)⁺. Fraction C (11 mg, 8.5%, β -anomer) was N^α -(9-fluorenylmethoxycarbonyl)-*O*-(3,4,6-tri-*O*-acetyl-2-azido-2-deoxy- β -D-galactopyranosyl)-L-serine pentafluorophenyl ester. R_f 0.43 (1:1 hexanes–EtOAc). ^1H NMR, (300 MHz, CDCl_3): δ 7.77, 7.61, 7.41, 7.31 (8H, Ar–H), 5.88 (d, 1H, $J_{\text{NH}-\text{CH}^\alpha}$ 8.7 Hz, NH), 5.34 (dd, 1H, $J_{4,5}$ 0.9 Hz, H -4), 4.99 (m, 1H, CH^α), 4.81 (dd, 1H, $J_{3,4}$ 3.3 Hz, H -3), 4.58 (dd, 1H, $J_{\text{CH}^\alpha-\text{CH}^\beta}$ 3.0 Hz, CH^β), 4.46 (m, 2H, Fmoc– CH_2), 4.42 (d, 1H, $J_{1,2}$ 8.1 Hz, H -1, diagnostic of β), 4.26 (t, 1H, J_1 6.9 Hz, J_2 7.2 Hz, Fmoc–CH), 4.03–4.16 (m, 2H, H -6), 3.99 (dd, 1H, $J_{\text{CH}_a^\beta-\text{CH}_b^\beta}$ 10.2 Hz, CH_b^β), 3.83 (m, 1H, H -5), 3.73 (dd, 1H, $J_{2,3}$ 10.8 Hz, H -2), 2.17, 2.08, 2.03 (3s, 9H, COCH_3). ESIMS: m/z 845.2 $[\text{M}+\text{K}]^+$, 829.2 $[\text{M}+\text{Na}]^+$, 807.2 $[\text{M}+\text{H}]^+$.

4.7.2. Method B. Following Paulsen et al.,⁹ a solution of compound **11** (400 mg, 0.82 mmol) in abs dry 1:1 toluene– CH_2Cl_2 (4 mL), together with Ag_2CO_3 (500 mg, 1.81 mmol), AgClO_4 (69 mg, 0.33 mmol) and molecular sieves (1.1 g, 3 Å, powdered), was stirred at 25 °C for 1 h in dark and under dry N_2 atmosphere. A solution of compound **7** (420 mg, $\alpha:\beta$ = 1:5.5, 1.2 mmol) in dry 1:1 toluene– CH_2Cl_2 (30 mL) was added dropwise over 45 min. After 4 days, product isolation by regular silica gel chromatography provided three fractions: fraction A (**15**, 20 mg, 5%), fraction B (desired **13**, 152 mg, 23%), fraction C (37 mg, 5%, β -anomer).

4.8. N^α -(9-Fluorenylmethoxycarbonyl)-*O*-(3,4,6-tri-*O*-acetyl-2-azido-2-deoxy- α -D-galactopyranosyl)-L-threonine pentafluorophenyl ester (14**)**

4.8.1. Method A. Again following Levine and co-workers¹¹ a solution of **12** (245 mg, 0.48 mmol) in dry 1:1 toluene– CH_2Cl_2 (30 mL) was stirred with Ag_2CO_3 (300 mg, 1.1 mmol) and molecular sieves (0.85 g, 3 Å, powdered)

in the dark and under N_2 , at 20 °C for 1 h. Next, AgClO_4 (36 mg, 0.18 mmol) was added and stirring was continued under the same conditions for 20 min. Then, **6** (285 mg, 0.73 mmol) in dry 1:1 toluene– CH_2Cl_2 (10 mL) was added dropwise over 1 h and stirring was continued for 24 h. Product isolation was the same as described for the preparation of **13**. Two fractions (R_f A = 0.73; R_f B = 0.33, 1:1 hexanes–EtOAc) were obtained by standard silica gel chromatography. Fraction A **16** (6 mg, 3%) was Fmoc–dehydrothreonine pentafluorophenyl ester. ^1H NMR (500 MHz, CDCl_3): δ 7.77 (d, 2H, $J_{3,4}$ 7.5 Hz, Ar–H-4), 7.60 (d, 2H, $J_{1,2}$ 7.2 Hz, Ar–H-1), 7.41 (m, 2H, Ar–H-3), 7.34 (m, 2H, Ar–H-2), 7.22 (q, 1H, $J_{\text{CH}-\text{CH}_3}$ 7.2 Hz, CH), 6.16 (br, 1H, NH), 4.51 (d, 2H, J 6.9 Hz, Fmoc– CH_2), 4.27 (t, 1H, Fmoc–CH), 1.91 (t, 1H, CH_3). ESIMS: m/z 512.1 $[\text{M}+\text{Na}]^+$. Fraction B was further purified by normal-phase preparative HPLC and gave the enantiopure title product **14** (110 mg, 28%, t_R 39.4 min), which was also purified by medium-pressure silica gel chromatography.⁹ ^1H NMR (500 MHz, CDCl_3):^{9,11} δ 7.77, 7.63, 7.40, 7.32 (8H, Ar–H), 5.85 (d, 1H, $J_{\text{NH}-\text{CH}^\alpha}$ 9.0 Hz, NH), 5.48 (d, 1H, $J_{3,4}$ 3.0 Hz, H -4), 5.31 (dd, 1H, $J_{2,3}$ 11.0 Hz, H -3), 5.18 (d, 1H, $J_{1,2}$ 3.6 Hz, H -1, diagnostic of α), 4.78 (dd, 1H, $J_{\text{CH}^\alpha-\text{CH}^\beta}$ 2.0 Hz, CH^β), 4.59 (m, 1H, CH^β), 4.41–4.51 (m, 2H, Fmoc– CH_2), 4.28–4.31 (m, 2H, H -5, Fmoc–CH), 4.12 (dd, $J_{5,6}$ 6.0 Hz, J_{6a-6b} 1.5 Hz, 2H, H -6), 3.77 (dd, 1H, H -2), 2.17, 2.08, 2.06 (3s, 9H, COCH_3), 1.46 (d, $J_{\text{CH}^\beta-\text{CH}_3}$ 6.0 Hz, 3H, CH_3). ESIMS: m/z 843.2 $[\text{M}+\text{Na}]^+$, 821.2 $[\text{M}+\text{H}]^+$. The β -anomer (15 mg, 3%, t_R 45.9 min) was also obtained by normal-phase preparative HPLC. ^1H NMR (500 MHz, CDCl_3): δ 4.53 (d, $J_{1,2}$ 7.8 Hz, H -1), diagnostic of β . ESIMS: m/z 843.2 $[\text{M}+\text{Na}]^+$, 821.2 $[\text{M}+\text{H}]^+$. (Additional NP-HPLC spectra are shown in the Supplementary data.)

4.8.2. Method B. Again following Paulsen et al.,⁹ a solution of compound **12** (385 mg, 0.76 mmol) in abs dry 1:1 toluene– CH_2Cl_2 (20 mL), together with Ag_2CO_3 (470 mg, 1.71 mmol) and molecular sieves (1.3 g, 3 Å, powdered) were stirred at 25 °C for 1 h in the dark and under a dry N_2 atmosphere. Then AgClO_4 (57 mg, 0.28 mmol) and compound **7** (398 mg, $\alpha:\beta$ = 1:5.5, 1.14 mmol) in dry 1:1 toluene– CH_2Cl_2 (10 mL) were added. After 3 days, the reaction was quenched by adding CH_2Cl_2 (40 mL) and filtered over dry Celite (~4 g). The filtrate was washed with 5% aq NaHCO_3 (3×10 mL) and water (2×10 mL), and then dried (Na_2SO_4). Following solvent evaporation, the sample was redissolved in EtOAc and applied to a regular silica gel column (15 \times 3 cm), which was eluted with 4:1 hexanes–EtOAc to provide two fractions. Fraction A was **16** (14 mg, 4%). Fraction B was further purified by normal-phase preparative HPLC and gave the enantiopure title product **14** (165 mg, 27%) and the β -anomer (20 mg, 3%).

4.9. ^1H NMR of *N*-acetyl-3,4,6-tri-*O*-acetyl-2-azido-2-deoxy- α -D-galactopyranosylamine (**5**) in the presence of LiBr, LiI, or NaI

LiBr (24 mg, 0.28 mmol) was suspended in a solution of compound **5** (20 mg, 53.7 μmol) in CD_3CN (1 g) with stirring, at 25 °C. Aliquots were taken for ^1H NMR spectroscopic (300 MHz) evaluation in situ: (a) Before adding LiBr. ^1H NMR data was in accordance with that reported before.¹³ (b) After 3 h: δ (ppm) 9.05 (d, 1H, $J_{\text{NH,H1}}$ 9.9 Hz, NH), 5.86–5.93 (m, 2H, *H*-1, *H*-3), 5.40 (d, 1H, $J_{3,4}$ 3.0 Hz, *H*-4), 5.49 (t, 1H, J_{a} 6.3 Hz, J_{b} 6.0 Hz, *H*-5), 4.22 (q, $J_{1,2}$ 5.7 Hz, $J_{2,3}$ 11.4 Hz, 1H, *H*-2), 3.99–4.11 (m, 2H, *H*-6), 2.18, 2.14, 2.04, 2.02 (4s, 12H, 4CH₃). (c) The reaction was quenched by adding CH_2Cl_2 , following which the mixture was concentrated to provide the organic product as a residue, which was then dissolved in CD_3CN . ^1H NMR data was in accordance with that reported before.¹³ The procedure for treatment with LiI (50 mg, 0.37 mmol) was the same as that of LiBr: (b) After 20 min: δ 8.52 (d, 1H, $J_{\text{NH,H1}}$ 9.6 Hz, NH), 5.83 (q, $J_{1,2}$ 5.7 Hz, 1H, *H*-1), 5.68 (dd, 1H, $J_{2,3}$ 11.3 Hz, *H*-3), 5.36 (dd, 1H, $J_{3,4}$ 3.3 Hz, *H*-4), 4.42 (t, J_{a} 6.0 Hz, J_{b} 6.6 Hz, 1H, *H*-5), 4.26 (q, 1H, *H*-2), 4.03 (m, 2H, *H*-6), 2.18, 2.13, 2.01, 2.00 (4s, 12H, 4CH₃). The procedure for treatment with NaI (40 mg, 0.27 mmol) was the same as that of LiBr. (b) After 20 min: ^1H NMR (300 MHz, CD_3CN): δ 8.01 (d, 1H, $J_{\text{NH,H1}}$ 9.6 Hz, NH), 5.84 (q, $J_{1,2}$ 5.7 Hz, 1H, *H*-1), 5.60 (dd, 1H, $J_{2,3}$ 11.4 Hz, *H*-3), 5.38 (dd, 1H, $J_{3,4}$ 3.3 Hz, *H*-4), 4.32 (t, J_{a} 6.0 Hz, J_{b} 6.6 Hz, 1H, *H*-5), 4.23 (q, 1H, *H*-2), 4.06 (m, 2H, *H*-6), 2.13, 2.09, 2.01, 2.00 (4s, 12H, 4CH₃).

4.10. X-ray data collection, solution, and refinement of compound **5**

4.10.1. Data collection. A crystal (approximate dimensions 0.20 \times 0.15 \times 0.10 mm³) was placed onto the tip of a 0.1 mm diameter glass fiber and mounted on a Bruker SMART Platform CCD diffractometer for a data collection at 173(2) K. A preliminary set of cell constants was calculated from 66 reflections harvested from three sets of 20 frames. The data collection was carried out using Mo K α radiation (graphite monochromator) with a frame time of 30 s and a detector distance of 4.90 cm. A randomly oriented region of reciprocal space was surveyed to the extent of one sphere and to a resolution of 0.77 Å. Final cell constants were calculated from 3813 strong reflections from the actual data collection after integration (SAINT).²⁷ The intensity data were corrected for absorption and decay (SADABS).²⁸ Additional crystal and refinement information has been compiled (Table 1).

4.10.2. Structure solution and refinement. The structure was solved using SHELXS-97²⁷ and refined using SHELXL-

97.²⁹ The space group $P2_1$ was determined based on systematic absences and intensity statistics. A direct-methods solution was calculated, which provided all nonhydrogen atoms from the E-map. All nonhydrogen atoms were refined with anisotropic displacement parameters. Hydrogen atoms were placed in ideal geometrical positions in a standard riding model, except that methyl torsion angles were refined. All hydrogen atoms were refined with relative isotropic displacement parameters relative to the host atom. The final full matrix least squares refinement converged to $R1 = 0.0396$ and $wR2 = 0.0977$ (F^2 all data).

Acknowledgements

We thank Professor Gary R. Gray for critical reading of the manuscript and William W. Brennessel of the X-ray Crystallographic Laboratory of the Department of Chemistry at the University of Minnesota for assistance in solving the structure of **5**. An anonymous referee made several helpful suggestions, which are appreciated insofar as they guided revision of the manuscript. This work was supported by grant GM 66148 from the National Institute of Health.

Supplementary data

The supplementary crystallographic data for this paper is contained in CCDC 264154. These data can be obtained free of charge via www.ccdc.cam.ac.uk/data_request/cif, or by emailing data_request@ccdc.cam.ac.uk, or by contacting The Cambridge Crystallographic Data Centre, 12, Union Road, Cambridge CB2 1EZ, UK; fax: +44 1223 336033.

NMR spectra of compounds **2–8**, and **11–16**, as well as some additional Tables and Figures related to the X-ray crystallographic analysis of **5**, have been compiled (total 47 pages), and Supplementary data associated with this article can be found, in the online version at [doi:10.1016/j.carres.2005.02.029](https://doi.org/10.1016/j.carres.2005.02.029).

References

1. Van den Steen, P.; Rudd, P. M.; Dwek, R. A.; Opdenaker, G. *Crit. Rev. Biochem. Mol. Biol.* **1998**, *33*, 151–208.
2. Kunz, H. *Angew. Chem., Int. Ed. Engl.* **1987**, *26*, 294–308.
3. Sames, D.; Chen, X. T.; Danishefsky, S. J. *Nature* **1997**, *389*, 587–591.
4. Kuduk, S. D.; Schwarz, J. B.; Chen, X. T.; Glunz, P. W.; Sames, D.; Ragupathi, G.; Livingston, P. O.; Danishefsky, S. J. *J. Am. Chem. Soc.* **1998**, *120*, 12474–12485.
5. Hojo, H.; Nakahara, Y. *Curr. Protein Pept. Sci.* **2000**, *1*, 23–48.
6. Bielfeldt, T.; Peters, S.; Meldal, M.; Bock, K.; Paulsen, H. *Angew. Chem., Int. Ed. Engl.* **1992**, *31*, 857–859.

7. Lüning, B.; Norberg, T.; Tejbrant, J. *Glycoconjugate J.* **1989**, *6*, 5–19.
8. Peters, S.; Bielfeldt, T.; Meldal, M.; Bock, K.; Paulsen, H. *J. Chem. Soc., Perkin Trans. 1* **1992**, *9*, 1163–1171.
9. Paulsen, H.; Bielfeldt, T.; Peters, S.; Meldal, M.; Bock, K. *Liebigs Ann. Chem.* **1994**, *4*, 369–379.
10. Yule, J. E.; Wong, T. C.; Gandhi, S. S.; Qiu, D.; Riopel, M. A.; Koganty, R. R. *Tetrahedron Lett.* **1995**, *36*, 6839–6842.
11. Gururaja, T. L.; Ramasubbu, N.; Levine, M. J. *Lept. Sci.* **1996**, *3*, 79–88.
12. Liu, M.; Live, D.; Barany, G. *Chimica Oggi* **2004**, *22*, 30–34.
13. Lemieux, R. U.; Ratcliffe, R. M. *Can. J. Chem.* **1979**, *57*, 1244–1251.
14. Vargas-Berenguel, A.; Meldal, M.; Paulsen, H.; Bock, K. *J. Chem. Soc., Perkin Trans. 1* **1994**, *18*, 2615–2619.
15. Kunz, H.; Birnbach, S. *Angew. Chem., Int. Ed. Engl.* **1986**, *25*, 360–362.
16. Paulsen, H.; Peters, S.; Bielfeldt, T.; Meldal, M.; Bock, K. *Carbohydr. Res.* **1995**, *268*, 17–34.
17. Paulsen, H.; Richter, A.; Sinnwell, V.; Stenzel, W. *Carbohydr. Res.* **1978**, *64*, 339–362.
18. Broddefalk, J.; Nilsson, U.; Kihlberg, J. *J. Carbohydr. Chem.* **1994**, *13*, 129–132.
19. Srinivas, O.; Muktha, B.; Radhika, S.; Guru Row, T. N.; Jayaraman, N. *Carbohydr. Res.* **2004**, *339*, 1447–1451.
20. Rendleman, J. A. *Adv. Carbohydr. Chem.* **1966**, *21*, 209–270.
21. Angyal, S. J. *Pure Appl. Chem.* **1973**, *35*, 131–146.
22. Angyal, S. J. *Adv. Carbohydr. Chem. Biochem.* **1989**, *47*, 1–43.
23. Verchère, J. F.; Chapelle, S.; Xin, F.; Crans, D. C. *Prog. Inorg. Chem.* **1998**, *47*, 837–945.
24. Yano, S.; Mikata, Y. *Bull. Chem. Soc. Jpn.* **2002**, *75*, 2097–2113.
25. Somlai, C.; Lovas, S.; Forgó, P.; Murphy, R. F.; Penke, B. *Synth. Commun.* **2001**, *31*, 3633–3640.
26. Jansson, A. M.; Meldal, M.; Bock, K. *J. Chem. Soc., Perkin Trans. 1* **1992**, *13*, 1699–1707.
27. SAINT V6.2, Bruker analytical X-ray systems, Madison, WI, 2001.
28. Blessing, R. H. *Acta Crystallogr., Sect. A: Found Crystallogr.* **1995**, *51*, 33–38.
29. SHELXTL V6.10, Bruker Analytical X-ray Systems, Madison, WI, 2000.